KARYA ILHAM PUBLISHING
CONNECTING MINDS, BRIDGING IDEAS, INSPIRING READERS

Malaysian Journal on Composites Science and Manufacturing
Journal homepage:
https://karyailham.com.my/index.php/mjcsm/index
ISSN: 2716-6945

Optimization of Friction Stir Welding Parameters for Dissimilar Al1060–C11000 Joints using Hybrid Taguchi-GRA Technique

Kapil Dev[1], Hari Om[1*], Tilak Raj[1]

[1] Mechanical Engineering Department, J.C. Bose University of Science and Technology, YMCA, Faridabad, 121006, India

ARTICLE INFO

Article history:
Received 18 November 2025
Received in revised form 12 January 2026
Accepted 23 February 2026
Available online 30 March 2026

ABSTRACT

This research work presents a systematic investigation of friction stir welding (FSW) between aluminum (Al1060) and copper (C11000) using a D2 tool steel, with a focus on optimizing mechanical performance. Three key factors, i.e., shoulder diameter (18, 20, and 22 mm), tool rotational speed (800, 1000, and 1200 rpm), and welding speed (90, 120, and 150 mm/min) were selected based on prior studies and preliminary trials. L_9 Taguchi orthogonal array was employed to efficiently evaluate the effects of selected parameters on tensile and flexural strengths. Multi-response optimization was performed by combining Taguchi analysis with Grey Relational Analysis (GRA), and the relative significance of each parameter was quantified using analysis of variance (ANOVA). The optimal welding condition was identified as a 20 mm shoulder diameter, 1200 rpm rotational speed, and 90 mm/min welding speed, providing maximum tensile and flexural strengths of 145 MPa and 285 MPa, respectively. ANOVA results showed that welding speed is the most effective factor affecting tensile strength (49.5%) and flexural strength (55.8%). Microstructural analysis showed that the selected parameters could successfully inhibit the overgrowth of intermetallic compounds and facilitate the refining of SZ, thereby enhancing fracture characteristics and mechanical properties. The originality of this work is the Hybrid Taguchi–GRA–ANOVA scheme and microstructure validation for different Al–Cu dissimilar FSW, and its results provide practical clues to industrial process optimization, finally towards high-strength, reliable joints with reduced experimental cost and enhanced production efficiency.

Keywords:
Al–Cu Welding, Dissimilar Metal Joints, Intermetallic Compounds, Tensile and Flexural Strength, Taguchi Method, Grey Relational Analysis, ANOVA

1. Introduction

[*] *Corresponding author.*
E-mail address: hariomjcbose@gmail.com (Hari Om)
E-mail of co-authors: kp1823@gmail.com, tilakraj@jcboseust.ac.in

https://doi.org/10.37934/mjcsm.19.1.1331

Aluminium and copper are among the most frequently used metallic materials in modern automotive, electrical, and refrigeration industries. They both offer distinct advantages that make them essential in the engineering field. Aluminium and its alloys are highly adaptable, as they have low density, excellent corrosion resistance, and adequate mechanical strength. These properties of aluminium contribute to lightweight structures with long service life, making it highly suitable for applications where lighter weight is the primary priority, without sacrificing performance. Copper, in comparison, has exceptional electrical and thermal conductivity. These properties made copper the primary choice for refrigeration coils, bus bars, electrical wiring, and heat exchangers. When such two metals or their alloys are combined to form a single piece, such as bus bars or electrical connectors, the designer can take advantage of the supplementary benefits of both. For such materials, aluminium contributes to weight reduction and corrosion resistance, whereas copper ensures reliable electrical current conduction and heat transfer. This synergy gives overall performance and cost advantages that neither material can acquire independently.

Apart from these advantages, the direct joining of aluminium and copper has certain limitations. Traditional fusion welding processes often result in the formation of brittle intermetallic compounds (IMCs), such as Al_2Cu, which precipitate at the interface of welded joints during high-temperature welding. These intermetallic compounds, if thicker, lead to a sharp reduction in mechanical reliability. Additionally, the thermal expansion coefficients and melting temperatures of copper and aluminum differ significantly, which increases residual stresses during cooling. For crucial Al–Cu components, fusion welding is not appropriate due to the combination of brittle IMCs and thermal incompatibilities, which often lead to joint cracking, reduced ductility, and a short fatigue life.

To overcome such limitations, friction stir welding (FSW) has emerged as a reliable solid-state joining technique. Unlike fusion welding, Friction stir welding was first used as a joining process and patented by The Welding Institute (TWI) of the UK in 1991 [1]. FSW does not involve bulk melting by mechanically stirring materials in a plasticized state. The workpieces are softened without passing over their melting points. This is due to the frictional heat produced by the rotating tool, which consists of a specially made pin and a shoulder. The plasticized area is where material mixing occurs, resulting in a metallurgical bond and finely crafted grain structures. It is an environmentally friendly technique that leverages energy efficiency and versatility to provide a satisfactory combination of microstructure and mechanical properties in the assemblies [2]. During the FSW process, the material undergoes intense plastic deformation at elevated temperature, resulting in the formation of fine, equiaxed recrystallized grains [3], [4]. The degree of IMC formation is significantly reduced, and the thermal mismatch between copper and aluminum is better accommodated because FSW operates below the melting temperature. According to studies, FSW can produce Al–Cu joints with significantly higher tensile strength, ductility, and reliability than fusion welds when process parameters and tool design are carefully controlled [5, 12]. FSW is used in various industries, including aerospace [6, 9], automotive [7], and robotics [8].

However, careful optimization of process parameters is important for producing high-quality Al–Cu friction stir welds. Important parameters that significantly affect weld quality include tool shoulder diameter, rotational speed, and traverse speed. A lack of heat input can result in void formation or incomplete bonding, whereas excessive heat can lead to the formation of brittle IMC layers. The efficiency of material stirring and mixing at the dissimilar interface is also determined by the tool's geometry. Therefore, optimizing these parameters is a major focus of current research, and statistical and multi-objective methods are frequently used to systematically assess their effects.

This research explains how a structured experimental process is designed to address these challenges using a Taguchi L9 orthogonal array. The aluminium alloy (Al1060) and copper (C11000)

sheets were joined using FSW. D2 tool steel has been specifically chosen for the fabrication of the tool due to its high wear resistance and thermal stability. The Taguchi method provides an efficient experimental framework by allowing the systematic study of multiple factors along with a reduced number of trial runs. For the present research work, three factors, i.e., tool shoulder diameter, tool rotational speed, and welding speed, have been adopted, with each having three levels. Through the use of analysis of variance (ANOVA) and signal-to-noise (S/N) ratio calculations, the experimental design sought to not only quantify the welded joint's tensile and flexural characteristics under various conditions but also to demonstrate how these parameters affect mechanical performance.

Also, Grey Relational Analysis (GRA) is very effective when multiple performance objectives need to be analyzed. For a deeper evaluation, flexural strength and other performance parameters are required, as tensile strength alone is insufficient to assess weld quality in Al–Cu FSW. The optimal set of parameters can be accurately identified by combining several observations/results into a single grey relational grade (GRG).

In addition to mechanical testing, microstructural analysis was conducted to correlate performance with metallurgical properties. The main focus is to check the thickness and morphology of intermetallic layers at the joint, and the generation of voids in the stir zone. Previous research shows that thin, continuous IMC layers can lead to bonding, but higher growth rates compromise weld-joint performance [12, 23]. By analyzing cross-sections of joints under scanning electron microscopy (SEM), the links between process settings and mechanical outcomes can be established.

The novelty of this research work lies in its comprehensive approach. A combination of Taguchi design of experiments (DOE) and multi-response Grey Relation Analysis (GRA) provides a statistically robust framework for parameter optimization. Additionally, by correlating mechanical results with microstructural observations, this research provides insight into the fundamental mechanisms governing weld joint quality. The results of this research are intended to support ongoing efforts to develop durable Al–Cu joints for various electrical and thermal applications. Currently, energy efficiency and reduced weight are important factors across industries, from electric mobility to power distribution. To achieve reliable Al–Cu FSW, recent research has highlighted the need for advancements in IMC control tool design and real-time process monitoring [12, 13]. By providing experimental evidence linking metallurgical transformations, process conditions, and mechanical performance, the current work extends these suggestions.

2. Literature Review

2.1 FSW of Al–Cu metals or alloys

Previous literature addresses friction stir welding and friction stir spot welding of aluminium and copper. Li *et al.* [5] provided an early comprehensive review of FSSW between Al and Cu, documenting typical microstructures, mixing behaviors, and common defect types (voids, tunneling, and flash. Subsequent experimental studies on AA1060–C11000 confirm that heat input, tool geometry, and lateral offset critically influence IMC formation and joint strength [11, 23]. Micro- and macro-scale FSW (including μFSLW) studies indicate that thin-sheet Al–Cu joints are particularly sensitive to plunge depth, pin profile, and local heat flow [25].

2.2 Controlling Intermetallic Compounds

Intermetallic compounds with their known brittle properties, like $CuAl_2$ and Al_4Cu_9, are thermodynamically stable byproducts of Al–Cu diffusion. Their thickness and continuity at the Al–Cu interface govern whether they function as a thin bonding layer (i.e., advantageous) or as a brittle

zone (i.e., prone to cracking) [12, 20]. Models for predicting IMC thickness based on heat input and diffusion kinetics have been proposed [20], and it has been observed through experimental work that higher rotation speeds and longer dwell times typically result in higher IMC thickness, but they may also improve mixing and dispersion of Cu particles in the Al matrix if material flow is intense enough [12].

2.3 Tool material for FSW and its wear

The choice of tools and materials is crucial for dissimilar friction stir welding. Due to its superior tool life, D2 tool steel (a high-carbon, high-chromium, cold-work tool steel) is most commonly used. Also, it offers good wear resistance for medium-duty joining operations [22]. It has been observed that processing D2 tool steel using Friction Stir Processing (FSP) under certain conditions produces acceptable microstructures [19].

2.4 Process optimization: Taguchi and Grey Relational Analysis

Taguchi orthogonal arrays and Taguchi analysis offer the most economical strategy to investigate multi-factor parameter spaces. In multi-response optimization, Taguchi is frequently used in combination with Grey Relational Analysis (GRA), which combines several performance metrics into a single Grey Relational Grade (GRG) for optimization and ranking [10,21]. Taguchi analysis, when combined with GRA, always yields the optimal optimization parameters. Kumar *et al.* [14-18] use this hybrid technique to optimize parameters for the fabrication and characterization of various composites. Previous research works illustrate the efficacy of a hybrid combination of Taguchi and GR Analysis for optimizing tensile strength, hardness, and impact toughness in similar aluminium welding systems [10, 25].

2.5 Gap Analysis

Gaps still exist in the systematic correlation between Taguchi-driven multi-response optimization and detailed microstructural IMC quantification for Al1060–C11000 using D2 tools, despite numerous studies on Al–Cu FSW and FSSW. Furthermore, many studies focus on tensile characteristics, while fewer address flexural behavior in thin-sheet joints pertinent to bus-bar applications. By integrating Taguchi L9 and GRA analysis with tensile and flexural testing, this work fills this gap and offers suggestions applicable to industrial practice.

Although numerous studies have reported on friction stir welding of dissimilar Al–Cu joints, most prior work has focused on single-response optimization (in particular, ultimate tensile strength), with less attention paid to combined mechanical performance. On the contrary, the current work offers a comprehensive multi-response optimization of tensile and flexural strength for thin-sheet Al1060–C11000 dissimilar joints, which are direct parameters for electrical bus bars, connectors, and lightweight current-carrying elements.

Moreover, this research creatively combines Taguchi L9 experimental design with analysis of variance (ANOVA) and grey relational analysis (GRA) into a single framework for the balanced optimization of several mechanical properties as a whole, rather than the separate improvement of each property. Besides statistical optimization, the formed welding process is explained from metallurgical aspects, including control of heat input, behavior during material flow, suppression of intermetallic compounds (IMCs), and microstructural refinement within the stir zone, and the

observed mechanical properties. This statistical–metallurgical coupled interpretation clearly distinguishes our work from previous studies on the optimization of Al–Cu friction stir welding. The main objectives of this research work are:

- To measure the tensile and flexural properties of Al–Cu friction stir welding joints for nine different configurations.
- To examine the effect of tool shoulder diameter, rotational speed, and welding speed
- To implement Grey Relational Analysis for multi-objective optimization to verify the results of Taguchi analysis; and
- To correlate the weld joint performance with microstructural evolution.

3. Materials and Methods

3.1 Materials

Sheets of pure copper C11000 and pure aluminum Al1060 were chosen. In this present investigation, sheets of 3 mm thickness were used. Specimen edges were properly milled and degreased before welding to attain a proper weld joint.

3.2 Machine and Tool

The friction stir welding machine used for welding could monitor force and torque. Standardized methods for clamping and backing plates reduce heat loss and movement. Figure 1 shows the pictorial view of the FSW machine with fixtures.

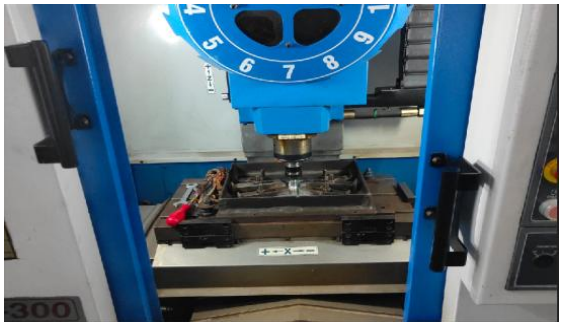

Fig. 1. FSW machine with fixtures

As shown in Figure 2, Heat-treated D2 tool steel, with enhanced wear resistance, was used as a welding tool. The tool shoulder diameters tested were 18, 20, and 22 mm; the pin profile was a threaded cylindrical/conical pin with a nominal pin length equal to the plate thickness minus 0.1–0.2 mm.

Fig. 2. D2 Steel Tool

3.3 Experimental Design

A Taguchi L_9 orthogonal array with three factors and three levels each was used. The selected three key factors are device shoulder diameter, tool rotational speed, and welding speed. The different levels for these three factors are 18 mm, 20 mm, and 22 mm; 800 rpm, 1000 rpm, and 1200 rpm; and 90 mm/min, 120 mm/min, and 150 mm/min, respectively. The selection of these levels is based on previous research and preliminary trials. The systematic combination of these factors in an L9 orthogonal array allows the overall number of experimental runs to be limited while preserving the statistical significance of the data.

Table 1
Factors with their corresponding levels for FSW

Factors ↓ Levels →	1	2	3
Shoulder diameter (mm)	18	20	22
Tool rotational speed (rpm)	800	1000	1200
Welding speed (mm/min)	90	120	150

After entering the input data into Minitab 19, the L9 Orthogonal Array shown in Table 2 was found to be most suitable for Taguchi analysis.

Table 2
L_9 Orthogonal Array

Run	Shoulder (mm)	Rotational Speed (rpm)	Welding Speed (mm/min)
1	18	800	90
2	18	1000	120
3	18	1200	150
4	20	800	120
5	20	1000	150
6	20	1200	90
7	22	800	150
8	22	1000	90
9	22	1200	120

The Friction stir welding starts with firmly clamping the aluminum and copper sheets. Proper clamping is necessary to prevent any movement during the welding process. Then, the non-consumable rotating D2 steel tool with a shoulder and a pin is positioned above the joint line between the two sheets. Then this rotating tool is pressed into the joints of the two sheets. Friction between this tool and the joint between two sheets generates localized heat, softening the material in the vicinity of the pin without melting it. After inserting the tool to the required depth, it is held there for a short period. By doing so, the material at the joint is heated and plasticized, making it sufficiently soft for stirring. The tool follows the joint line during forward motion, and at the same time, the pin stirs and mixes the softened material on both sides, while the shoulder forges the material behind the tool and adds more frictional heating, leading to a solid-state bond. Material from both the advancing and retreating sides flows around the pin due to the tool's rotation, mixing and solidifying in its wake, thereby developing a fine-grained microstructure in the weld zone. A fine-grained microstructure forms in the weld zone as material from the retreating and advancing sides flows around the pin from the tool's rotation, mixes, and solidifies in its wake. The tool is gradually withdrawn when it reaches the end of the weld joint and completes the welding. The tool is gradually removed as the weld approaches the joint's end. Figure 3 shows the initial, middle, and final stages of the first FSW-fabricated specimen.

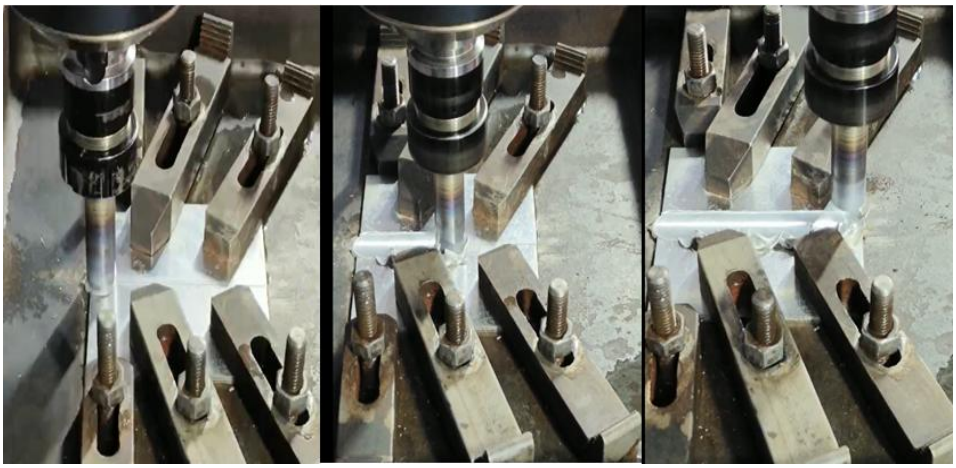

Fig. 3. Initial, middle, and final welding stages

After welding, three specimens for each of nine different runs, as per the Taguchi L9 orthogonal array, have been prepared for tensile testing using the ASTM D638 subsize geometry for thin sheets. Tensile tests were performed on a Universal Testing Machine with a constant crosshead speed of 2 mm/min. Figure 4 (a) shows three test specimens before the tensile tests.

Fig. 4 (a). Specimens for Tensile Testing (b). Specimens after Tensile Testing

Figure 4(b) shows images of the nine specimens tested under uniaxial tensile testing, and it presents the tensile-strength results for friction-stir-welded joints. Each specimen is clamped in a universal testing machine and loaded gradually in tension until fracture. Each sample will provide a stress–strain curve that reveals elastic deformation, yielding, plastic flow, and finally fracture. Based on the fracture location, found in the gauge region of each specimen, the weld zone is typically the weakest area relative to the base metal. While some samples exhibit brittle behavior (flat, sharp breaks), others show ductile behavior (significant necking and elongation). The observation of variation in fracture patterns across different samples reflects the effect of varying welding parameters on the microstructure and mechanical properties. This will help in identifying the optimal process parameters that lead to higher tensile strength and better joint quality.

The tensile strengths of the weldments are shown in Table 3. These are the average tensile strengths obtained from testing three specimens per run.

Table 3

Weldments tensile strengths

Run	Shoulder (mm)	Rotational Speed (rpm)	Welding Speed (mm/min)	Tensile Strength (MPa)
1	18	800	90	125
2	18	1000	120	118
3	18	1200	150	128
4	20	800	120	130
5	20	1000	150	120
6	20	1200	90	145
7	22	800	150	110
8	22	1000	90	140
9	22	1200	120	128

One method of testing materials is the bending test, which involves applying a load to determine the material's bending strength. ASTM D790 was used to conduct this test. Each specimen measured 150 mm in length, 10 mm in width, and 3 mm in thickness. The test was conducted with a constant load applied to the specimen, which was positioned on the UTM machine fixtures as depicted in Figure 5. Peak load values are calculated for each specimen. The flexural strength of various specimens can be determined using a formula based on the theory of the three-point bend test. The bending test, which evaluated the joint strength (bond strength) of the weld samples, was completed successfully.

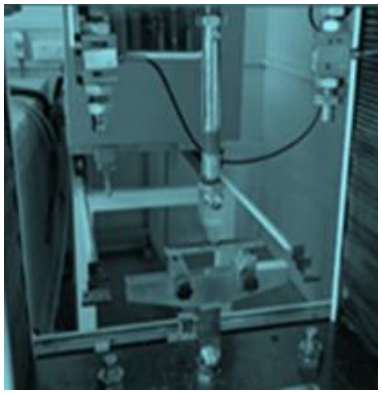

Fig. 5. Flexural Testing Set Up

The weldments Flexural strengths are shown in Table 4. These are the average values of the flexural strength observed after testing three specimens for each run.

Table 4

Weldments flexural strengths

Run	Shoulder (mm)	Rotational Speed (rpm)	Welding Speed (mm/min)	Flexural Strength (MPa)
1	18	800	90	240
2	18	1000	120	252
3	18	1200	150	247
4	20	800	120	245
5	20	1000	150	220
6	20	1200	90	285
7	22	800	150	200
8	22	1000	90	270
9	22	1200	120	250

3.4 Microstructural analysis

Microstructural characterization of the weld in a friction stir-welded (FSW) joint is crucial for understanding the joint's integrity and performance. Microstructures were observed on transverse-section samples prepared according to standard metallographic methods. The samples were initially cold-cast in epoxy resin and then ground incrementally with SiC abrasive papers of successively finer grain sizes. The specimens were polished using a fine abrasive alumina suspension and used for the mirror surface polishing.

The polished samples were etched with Keller's reagent to clearly show the microstructures and the Al–Cu interface. Analyses of the microstructure and fracture surface were carried out using an SEM with the appropriate accelerating voltage and working distance to achieve an acceptable resolution. The morphology of the fracture and the quality of the material flow through and at the interfaces in welded joints were qualitatively characterized using SEM examination.

3.5 Taguchi & Grey Relational Analysis

Taguchi analysis is a statistical optimization technique used to determine the effects of selected process parameters on response characteristics with a minimum number of experiments. For this research, the Taguchi method has been adopted to evaluate the effects of welding parameters on mechanical properties, including ultimate tensile strength (UTS) and flexural strength. Signal-to-Noise (S/N) ratios have been calculated for both types of responses by selecting the "larger-is-better" option, as higher mechanical strength is desired. The process's resilience to changes was evaluated by examining S/N ratios, which also enabled the identification of parameter settings that optimize mechanical performance. Additionally, an Analysis of Variance (ANOVA) has been performed on the S/N ratios to assess the contribution of each factor and determine which welding parameters have the greatest impact on the mechanical properties.

Whereas Taguchi analysis is effective for optimizing a single response, Grey Relational Analysis (GRA) allows simultaneous optimization of multiple responses, initially by normalizing the S/N ratios of the two responses to values between 0 and 1. Thereafter, the Grey Relational Coefficients (GRC) were calculated using a constant coefficient of 0.5 (commonly used in all GR Analysis), which balances data-point differentiation and sensitivity. Then, the Grey Relational Grades (GRGs) have been calculated for each experiment by taking the arithmetic mean of the GRCs for both responses, with equal weighting. A higher GRG value ensures the optimized performance of the process parameters with respect to both the responses, i.e., tensile and flexural strength. Grey Relation Analysis reduces a multi-response optimization problem to a single composite index.

4. Results

4.1 Raw mechanical data

The combined experimental results for tensile and flexural strength, obtained from nine runs, are shown in Table 5. To improve the results, the table above uses the average of three repeats per run (mean ± SD).

Table 5
Experimental results of Tensile and Flexural strength

Run	Tensile Strength (MPa)	Flexural Strength (MPa)
1	125	240
2	118	252
3	128	247
4	130	245
5	120	220
6	145	285
7	110	200
8	140	270
9	128	250

Three independent experiments were performed for each experimental condition, and the tensile and flexural strength values are presented as the mean of these replicates. The similar features of the measured responses across different repeatability runs provide fairly strong evidence of acceptable experimental reproducibility in parameter selection. The statistical analysis here is based on the average response value because of the relatively small number of repetitions in the Taguchi L9 design, rather than on full interval estimation.

4.2 Taguchi S/N Ratio Calculations (Larger-is-Better)

S/N ratios were calculated for each response using the larger-is-better formulation: S/N = -10 * log10 (mean(1/Y^2)). Table 6 lists S/N values for tensile and flexural responses.

Table 6
Experimental Runs with Measured Responses and S/N Ratios for two responses

Run	Tensile Strength (MPa)	Flexural Strength (MPa)	S/N (Tensile) dB	S/N (Flexural) dB
1	125	240	41.94	47.6
2	118	252	41.44	48.03
3	128	247	42.14	47.85
4	130	245	42.28	47.78
5	120	220	41.58	46.85
6	145	285	43.23	49.09
7	110	200	40.83	46.02
8	140	270	42.92	48.61
9	128	250	42.14	47.96

Table 7
Response Table for S/N Ratios (Larger is better) for Tensile Strength

Level	Shoulder (mm)	RPM	Weld Speed (mm/min)
1	47.83	47.14	48.44
2	47.91	47.83	47.92
3	47.54	48.30	46.91
Delta	0.37	1.17	1.54
Rank	3	2	1

Figure 6 shows the effect of shoulder diameter, rotational speed (RPM), and weld speed on the S/N ratios for tensile strength under the "larger-is-better" option. The graph indicates that shoulder diameter has a very mild effect, with higher performance at 20 mm. In contrast, RPM has a very strong positive effect, as shown in the S/N plot: higher speeds significantly improve the mean S/N ratio, with an optimal range of 1200 RPM. The effect of welding speed is most noticeable: the highest S/N ratio is obtained at a low speed of 90 mm/min, and performance gradually declines as the speed increases to 150 mm/min. According to the S/N plot, the optimal combination for performance is a 20 mm shoulder, 1200 RPM, and a 90 mm/min weld speed.

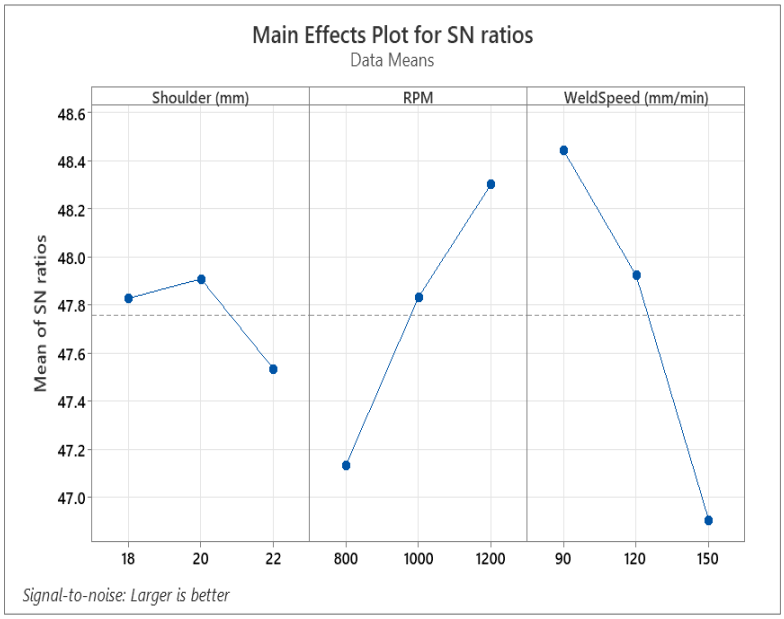

Fig. 6. Graph for S/N Ratios for Tensile Strength

Table 8
Response Table for S/N Ratios (Larger is better) for Flexural Strength

Level	Shoulder (mm)	RPM	Weld Speed (mm/min)
1	47.83	47.14	48.44
2	47.91	47.83	47.92
3	47.54	48.30	46.91
Delta	0.37	1.17	1.54
Rank	3	2	1

Figure 7 shows the effect of shoulder diameter, rotational speed (RPM), and weld speed on the S/N ratios for flexural strength under the "larger-is-better" criteria. Figure 7 shows that, likewise to that of the tensile test S/N plot, shoulder diameter have a very mild effect, with higher performance at 20 mm. But the RPM has a very strong positive effect, which is visible in the S/N graph, in that the higher speeds significantly improve the mean S/N ratio, at an optimal range of 1200 RPM. For welding speed, the highest S/N ratio is obtained at a low welding speed of 90 mm/min, and the performance gradually declines as the speed rises to 150 mm/min. Again, as per the S/N plot of flexural strength,

the optimal combination for best results is a 20 mm shoulder, 1200 RPM, and a 90 mm/min weld speed.

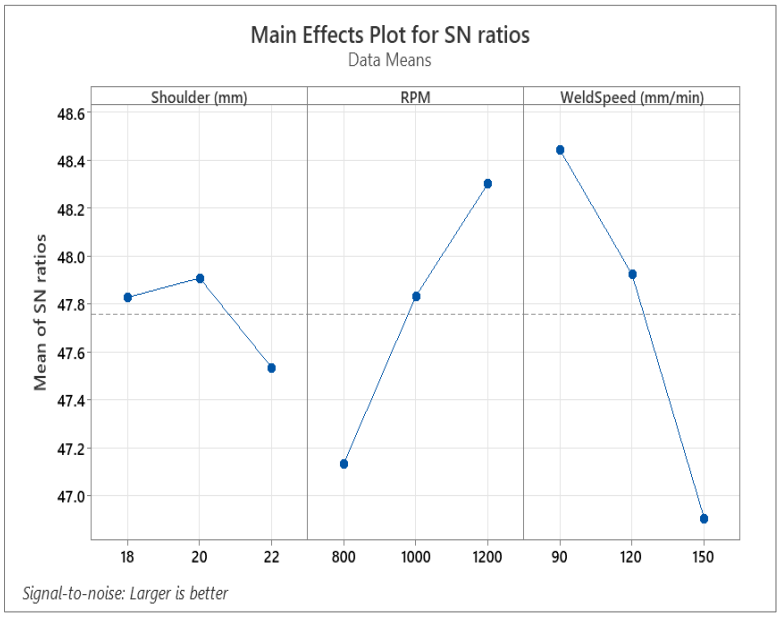

Fig. 7. Graph for S/N Ratios for Flexural Strength

4.3 ANOVA of tensile and flexural strength

ANOVA has been performed to estimate the percentage contribution of each factor for both the responses, i.e., tensile and flexural strength.

4.3.1 ANOVA results for S/N (Tensile)

Table 9 presents the ANOVA analysis of the S/N ratios to estimate the percentage contribution of each factor to tensile strength.

Table 9
ANOVA analysis for Tensile Strength (S/N ratio)

Source	Sum of Squares	d. f.	F-value	p-value	% Contribution
Shoulder	0.449	2	0.648	0.607	10.42%
RPM	1.034	2	1.493	0.401	23.99%
Speed	2.136	2	3.083	0.245	49.53%
Residual	0.693	2	–	–	16.06%

From the ANOVA analysis table, it has been observed that weld speed is the most influential factor for the tensile strength of the weld joint, accounting for approximately 49.5% of the variation, followed by RPM (24%) and shoulder diameter (10.4%). Also, none of the used parameters are statistically significant at the 95% confidence level; however, weld speed dominates tensile strength, underscoring its crucial role in controlling joint quality.

4.3.2 ANOVA results for S/N (Flexural)

Table 10 presents the ANOVA analysis of the S/N ratios to estimate the percentage contribution of each factor to tensile strength.

Table 10
ANOVA analysis for Flexural Strength (S/N ratio)

Source	Sum of Squares	d.f.	F-value	p-value	% Contribution
Shoulder	0.236	2	0.418	0.705	3.64%
RPM	2.067	2	3.654	0.215	31.84%
Speed	3.624	2	6.406	0.135	55.81%
Residual	0.566	2	–	–	8.71%

The one-way analysis of variance (ANOVA) results showed that none of the process parameters was statistically significant at the 95% confidence level, since all p-values were greater than 0.05. The effect is primarily due to the limited degrees of freedom in the Taguchi L9 orthogonal array, which limits the statistical power for hypothesis testing. However, the ANOVA result provides useful information through percentage contributions, from which we can gain an impression of the relative effects of individual parameters on the responses.

4.3 Grey Relational Analysis (GRA)

The values of the two responses have been normalized (larger-is-better) to the range 0-1. Deviations and Grey Relational Coefficients (GRCs) have been calculated using a constant coefficient ζ = 0.5. Grey Relational Grades (GRGs) have been computed as the mean of the GRCs (equal weighting). Table 11 shows the normalized values, deviation, GRC, and GRG.

Table 11
Normalization, Deviation, GRC, and GRG for each run (higher GRG = better)

Run	Normalized Values (Tensile)	Normalized values (Flexural)	Devi. Seq. (Tensile)	Devi. Seq. (Flexural)	GRC Tensile	GRC Flexural	GRG
1	0.4286	0.4706	0.5714	0.5294	0.4667	0.486	0.476
2	0.2286	0.6118	0.7714	0.3882	0.3933	0.563	0.478
3	0.5143	0.5529	0.4857	0.4471	0.5072	0.528	0.517
4	0.5714	0.5294	0.4286	0.4706	0.5385	0.515	0.526
5	0.2857	0.2353	0.7143	0.7647	0.4118	0.395	0.403
6	1.0000	1.0000	0.0000	0.0000	1.0000	1.0000	1.0000
7	0.0000	0.0000	1.0000	1.0000	0.3333	0.333	0.333
8	0.8571	0.8235	0.1429	0.1765	0.7778	0.739	0.758
9	0.5143	0.5882	0.4857	0.4118	0.5072	0.548	0.527

The GRA table shows that, among nine experimental runs, Run 6 achieved the highest grey relational grade of 1, indicating the best performance in both tensile and flexural strength, suggesting that the parameter combination used in Run 6 provides the most balanced and optimal mechanical properties. Runs 4 and 9 have moderate GRG values of 0.526-0.527, indicating satisfactory but not acceptable results. The GRG value for Run 8 is 0.758, showing a strong performance for both responses. Furthermore, Run 7 has the lowest GRG valve at 0.333, reflecting the lowest combined performance for both responses.

5. Discussion

Tensile and flexural testing of nine distinct process parameter combinations, as designed by the Taguchi L9 orthogonal array, has been used to assess the mechanical behaviour of aluminium–copper friction stir-welded (FSW) joints. The measured tensile and flexural strengths varied from 110 to 145 MPa and 200 to 285 MPa, respectively. These results showed a strong dependence on welding speed, rotational speed, and tool shoulder diameter.

5.1. Taguchi Analysis of Tensile and Flexural Strength

The larger-is-better criterion was used to calculate the signal-to-noise (S/N) ratios for tensile and flexural strengths. The graphs for S/N ratios show the effect of the three selected process parameters, i.e. shoulder diameter, rotational speed (RPM), and weld speed, on the joint performance. Among these factors, weld speed has the greatest effect, with the highest S/N ratio at 90 mm/min and a sharp decline at 150 mm/min, indicating that a lower weld speed is best for achieving optimal joint strength. This suggests that while higher traverse speeds shorten the tool-workpiece interaction time and can lead to defects such as voids or inadequate bonding, lower traverse speeds encourage adequate heat input and material mixing. RPM is the next influential parameter, whose performance improves steadily from 800 to 1200 rpm, at which the maximum S/N ratio is obtained. It has been found that at higher RPMs, the plastic deformation, stirring efficiency, and heat generation. Also, the strength increased steadily as RPM increased. Excessive RPM, however, may increase the formation of thick intermetallic compounds (IMC). Although shoulder diameter has the least impact, 20 mm offers a slightly higher S/N ratio than 18 and 22 mm. Lower shoulder diameter provides insufficient heat, while excessive flash formation may be provided by employing the largest shoulder diameter.

The Taguchi analysis indicates that the ideal set of parameters for a perfect weld joint is a 20 mm shoulder diameter, a 1200 rpm rotational speed, and a 90 mm/min weld speed. So, from this analysis, it has been observed that shoulder diameter has a relatively small impact on joint quality, whereas weld speed and RPM dominate.

5.2 Grey Relational Analysis (GRA)

Since both tensile and flexural strength are critical in assessing joint quality, Grey Relational Analysis was performed for multi-response optimization. The Grey Relational Analysis (GRA) result is based on the normalized values of tensile and flexural strength, and it clearly reveals the relative performance of each experimental run. Normalization values followed by deviation sequences have been calculated for the two responses. Then, using a distinguishing coefficient of 0.5, the Grey Relational Coefficients (GRCs) have been computed. Finally, the Grey Relational Grades (GRGs) have been obtained by averaging the two GRCs for tensile and flexural strength. These GRGs provide a single performance index for multi-objective optimization. GRA shows that Run 6 exhibits the highest GRG value of 1 and that this experimental run has the best combined tensile and flexural performance among all trials. Following Run 6 are Runs 8 and 9, both of which exhibit strong performance with GRG values of 0.758 and 0.527, respectively. Runs 1-4 have moderate GRG values

ranging from 0.476 to 0.526. With GRG values of 0.403 and 0.333, respectively, runs 5 and 7 have the lowest rank and exhibit subpar tensile and flexural performance. Finally, Grey Relation Analysis indicates that Run 6 with 20 mm shoulder diameter, 1200 rpm rotational speed, and 90 mm/min weld speed, is the optimal parameter setting for balancing both mechanical properties.

The GRA results, which strongly support Taguchi's findings, thus highlight the importance of low welding speed and high rotational speed in enhancing joint strength.

5.3. ANOVA Results

Although the ANOVA analysis at the 95% confidence level does not show statistical significance, the observed trends in S/N ratios and percent contribution values clearly indicate that this model identifies welding speed as the most influential factor, followed by rotational speed and tool shoulder diameter. Interpretation of this sort, based on trends such as the above, is standard practice in Taguchi-based optimization studies with limited CRD's for screening, because the focus is often on parameter ranking and process optimization rather than on inferential statistics.

The present findings are considered trend-significant rather than statistically significant; this potential limitation was explicitly addressed to preclude overinterpretation of statistical results. Although the present research ensures repeatability by averaging repeated measurements within each experimental run, confidence interval estimation and statistical spread plots are absent in some previous reports. Such a conditional analysis can be considered in future research using a larger experimental dataset to provide more comprehensive quantification of variability and uncertainty.

5.4 Heat Input Considerations

In friction stir welding, the effective heat input is predominantly controlled by the tool rotation speed and welding (travel) speed, which collectively influence the generation of frictional heat and the plasticization of the material. Direct calorimetric measurement of heat input was beyond the scope of the present experimental setup.

Adequate plasticizing time and good material flow in the stir zone were achieved due to lower welding speeds and moderate–high rotational speeds in this study. This was beneficial for forming sound joints and for suppressing Al–Cu interface IMC growth. On the other hand, excessively high welding speeds shortened the tool–material interaction time, resulting in insufficient heat generation and a lower degree of consolidation, possibly creating voids or areas with weak bonding.

The results indicated that the ideal heat input is crucial to the trade-off among material flow, microstructural refinement, and IMC control, which directly affects the tensile and flexural performance of dissimilar Al1060–C11000 Friction Stir Welded joints.

5.5 Microstructural Correlation

The microstructural examination in this research is primarily based on SEM characterization of a fractured surface, which provides an indication of the prevailing failure modes for each process parameter combination. Direct zone-specific imaging of the stir zone (SZ), thermo-mechanically affected zone (TMAZ), and heat-affected zone (HAZ), as well as quantitative measurements of

intermetallic compound (IMC) thickness, were not conducted; however, there exists an analytical relationship between observed mechanical responses and known metallurgical behaviours reported in the literature. SEM images were acquired at appropriate magnifications, with corresponding scale bars as indicated in the figure. These SEM images, displayed in Figures 11 (a, b), show the fracture surfaces of tensile-tested friction stir welded (FSW) joints.

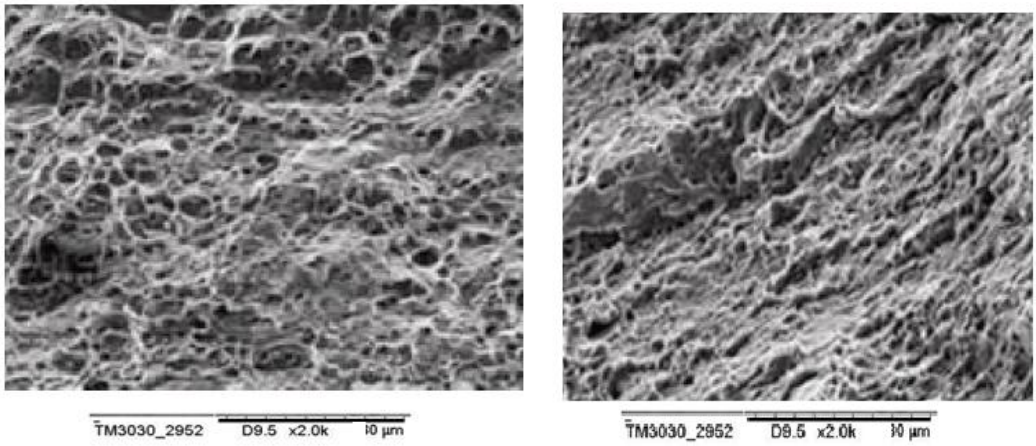

(a) (b)

Fig. 11. (a, b) SEM images of fracture surfaces of tensile-tested (FSW) joints

Figure 11(a) shows the SEM image of the fracture surface of one of the tensile specimens, and it has been observed that the surface is highly porous and dimpled, with several deep cavities. This type of morphology is found in ductile fracture, where micro-void nucleation, growth, and coalescence exist. The presence of interconnected dimples indicates that plastic deformation occurred before the final fracture, demonstrating that the weld metal still retains some ductility. On the other hand, the uniform distribution of dimples means proper bonding at the stir zone. But the depth and size of the voids indicate the localized weak regions.

Figure 11(b), for another test specimen, shows that the surface has a more elongated, fibrous structure, with tear patterns and ridges. The elongated characteristics, which are indicative of ductile tearing, imply plastic flow under tensile loading. Compared with the image in Figure 11(a), this surface appears rougher and more uneven, indicating that fracture initiation occurs in the weaker regions (probably at the weld interface). A transition region is visible in the finer distribution of dimples mixed with tearing ridges. It is still ductile, but it may be influenced by microstructural heterogeneity from the FSW process.

Both images confirm that the welds primarily failed by ductile fracture, with dimple rupture as the dominant mechanism. Differences in intermetallic compound distribution, local heat input, or weld parameters could all contribute to the differences in surface morphology between the two samples.

Economically optimal parameter combinations for sensible heat input should facilitate stir-zone grain refinement and IMC control at the Al–Cu interface, thereby increasing joint strength. On the other hand, excessive heat input can promote IMC growth and embrittlement, while insufficient heat input may result in inadequate material mixing and lower-quality interfacial bonding. The observed

fracture morphologies are consistent with the expected microstructural responses, providing a mechanistic interpretation of the mechanical response even without direct IMC quantification.

It has been found that enough frictional heat is produced at a combination of higher tool rotational speeds and lower welding speeds to enable dynamic recrystallization in the stir zone, resulting in fine equiaxed grains and robust metallurgical bonding. However, too-fast speeds reduce heat input, leading to void formation or insufficient mixing.

The abrasion behavior trends are similar to those reported in previous studies of dissimilar Al–Cu friction stir welded joints. A number of researchers have also reported that lower welding speeds and moderate rotational velocity result in sufficient heat input, better material flow, and increased joint strength by controlling unwanted intermetallic compound (IMC) formation at the Al–Cu interface. The current findings show a consistent trend: optimized parameter combinations and strengths improve tensile and flexural properties, revealing the ductile nature of fracture.

In contrast, work at higher speeds has reported inadequate mixing and internal defects, resulting in lower joint efficiency. A similar decrease in mechanical properties was observed in the current work at higher welding speeds and can be attributed to reduced interaction time between the tool and the material, leading to insufficient plasticization.

In addition, the literature reports that high heat input may accelerate IMC growth and induce brittle fracture modes. The observed crack morphologies in the current work at high heat input, in conformance with these observations, support the metallurgical interpretation of these results. In general, the agreement between the present observations and the literature trends indicates that the applied Taguchi–GRA optimization procedure is reliable.

6. Conclusions

This research work systematically investigated the friction stir welding of Al1060 and C11000 copper sheets using a hybrid combination of Taguchi Analysis (L_9 orthogonal array) and Grey Relational Analysis. The key findings from this research work are as follows:

- Mechanical properties were significantly impacted by the process variables that were chosen. The range of tensile and flexural strengths was 110–145 MPa and 200–285 MPa, respectively.
- According to Taguchi S/N ratio analysis, welding speed is the most crucial factor, followed by RPM, with shoulder diameter carrying the minimum effect.
- According to Grey Relation Analysis, the best final performance was attained for the 6th experimental Run i.e., for 20 mm shoulder diameter, 1200 RPM, and 90 mm/min weld speed with tensile strength 145 MPa and Flexural Strength as 285 MPa.
- ANOVA results quantified the factor contributions and indicated that the welding speed was the most important factor in controlling weld joint quality, both tensile (49.5%) and flexural (55.8%) strength.
- The best parameters according to microstructural reasoning restrict the growth of intermetallic compounds and encourage fine-grained stir zone structures, which are directly associated with better mechanical performance. In this work, the focus is on mechanical behavior and fracture surface observation in dissimilar Al–Cu FSW joints. The quantitative

description of intermetallic compound thickness and the detailed zone-wise microstructural observation (SZ, TMAZ, and HAZ) are not the focus of this work, but are recognized as study limitations.

This research work provides a hybrid, statistically precise framework for process optimization and useful insights for fabricating strong, durable Al–Cu FSW joints. These joints have significant potential for lightweight electrical and thermal applications, such as connectors, heat exchangers, and bus bars.

Acknowledgement
This research is not funded by any institute or agency. Also, we are thankful to Dr. Anil Kumar, Assistant Professor at DSEU, New Delhi, for his assistance with the computational work.

References

[1] W. M. Thomas, E. D. Nicholas, J. C. Needham, M. G. Murch, P. Temple-Smith, and C. J. Dawes, Friction Stir Welding, International Patent Application No. PCT/GB92/02203 and GB Patent Application No. 9125978.8 (December 1991).
[2] Y. C. Chen and K. Nakata, "Effect of the Surface State of Steel on the Microstructure and Mechanical Properties of Dissimilar Metal Lap Joints of Aluminum and Steel by Friction Stir Welding," *Metallurgical and Materials Transactions A* 39, no. 8 (2008): 1985–1992, https://doi.org/10.1007/s11661-008-9523-4
[3] C. G. Rhodes, M. W. Mahoney, W. H. Bingel, R. A. Spurling, and C. C. Bampton, "Effects of Friction Stir Welding on Microstructure of 7075 Aluminium," *Scripta Materialia* 36, no. 1 (1997): 69–75, https://doi.org/10.1016/S1359-6462(96)00344-2
[4] S. Benavides, Y. Li, L. E. Murr, D. Brown, and J. C. McClure, "Low-Temperature Friction-Stir Welding of 2024 Aluminum," *Scripta Materialia* 40, no. 8 (1999): 809–815.
[5] M. Li, C. Zhang, D. Wang, L. Zhou, D. Wellmann, and Y. Tian, "Friction Stir Spot Welding of Aluminum and Copper: A Review," *Materials* 13, no. 1 (2019): 156, https://doi.org/10.3390/ma13010156
[6] G. Wang, Y. Zhao, and Y. Hao, "Friction Stir Welding of High-Strength Aerospace Aluminum Alloy and Application in Rocket Tank Manufacturing," *Journal of Materials Science & Technology* 34, no. 1 (2018): 73–91.
[7] P. J. Hartley, D. E. Hartley, and A. McCool, "FSW Implementation on the Space Shuttle's External Tank," Document ID: 20010069325. Lockheed Martin Space Systems – Michoud Operations, NASA Marshall Space Flight Center (2001).
[8] S. Kallee, "Application of Friction Stir Welding in the Shipbuilding Industry," in Lightweight Construction (Cambridge, UK: The Royal Institution of Naval Architects, TWI, 2000), 25–25.
[9] C. B. Smith, J. F. Hinrichs, and W. A. Crusan, "Robotic Friction Stir Welding: The State of the Art," in Proceedings of the Fourth International Symposium on Friction Stir Welding (2003): 14–16.
[10] S. S. Abdelhady, R. E. Elbadawi, and S. H. Zoalfakar, "Multi-Objective Optimization of FSW Variables on Joint Properties of AA5754 Aluminum Alloy using Taguchi Approach and Grey Relational Analysis," *The International Journal of Advanced Manufacturing Technology* 130 (2024): 4235–4250, https://doi.org/10.1007/s00170-024-12969-2
[11] K. Devarajan *et al*., "Experimental Investigation and Characterization of Friction Stir Welds Between AA1060 and Copper," *ACS Omega* (2023), https://doi.org/10.1021/acsomega.3c02706
[12] M. Elyasi, A. Zarei-Hanzaki, and M. Sattar, "The Effect of Pin Thread on Material Flow and Mechanical Behaviour in Friction Stir Welding," *Heliyon* 9, no. 4 (2023): e14752, https://doi.org/10.1016/j.heliyon.2023.e14752
[13] M. I. A. Habba and M. M. Z. Ahmed, "Friction Stir Welding of Dissimilar Aluminum and Copper Alloys: A Review of Strategies for Enhancing Joint Quality," *Journal of Advanced Joining Processes* (2025): 100293, https://doi.org/10.1016/j.jajp.2025.100293
[14] A. Kumar, A. K. Chanda, and S. Angra, "Application of Hybrid Taguchi–GRA–PCA and ANOVA in Optimisation of Deformation Properties of Sandwich Structure," *International Journal of Nanotechnology* 18, no. 11–12 (2021): 951–967, https://doi.org/10.1504/IJNT.2021.119220
[15] A. Kumar, S. Angra, and A. K. Chanda, "Stress Properties Optimization of a Composite Sandwich Structure by Application of Hybrid Taguchi–GRA–PCA," *Journal of Engineering Research* (EMSME Special Issue) (2021): 203–216.

[16] A. Kumar, A. K. Chanda, and S. Angra, "Optimization of Stiffness Properties of Composite Sandwich using Hybrid Taguchi–GRA–PCA," *Evergreen: Joint Journal of Novel Carbon Resource Sciences & Green Asia Strategy* 8, no. 2 (2021): 310–317, https://doi.org/10.5109/4480708

[17] A. Kumar, B. Dahiya, and D. Grover, "Taguchi–GRA–PCA Approach: Optimizing Agricultural Waste Powder Epoxy Composite for Enhanced Strength using a Hybrid Method," *Evergreen* 11, no. 2 (2024): 713–721, https://doi.org/10.5109/7183347

[18] A. Kumar, R. Sharma, J. P. Supale, and G. S. Datar, "Development and Optimization of Agricultural Husk-Epoxy Composites: A hybrid Taguchi–GRA–PCA Approach for Enhanced Mechanical Performance," *Indian Journal of Environmental Protection* 45, no. 10 (2025): 882–890.

[19] Q. Liu, X. Chen, K. Liu, V. A. M. Cristino, *et al*., "Friction Stir Processing of M2 and D2 Tool Steels for Improving Hardness, Wear and Corrosion Resistances," *Surface and Coatings Technology* 481 (2024): 130609, https://doi.org/10.1016/j.surfcoat.2024.130609

[20] F. Momeni, "A New Model for Predicting the Thickness of Intermetallic Compounds in Dissimilar Welding," *Journal of Materials Science & Technology* 36, no. 2 (2020): 201–212.

[21] M.F. Mohamed, "Optimization of Friction Stir Welding Parameters using Taguchi-Based Grey Relational Analysis," *Journal of Manufacturing Processes* (2021).

[22] G. Mrudula, P. Bhargavi, and A. Krishnaiah, "Effect of Tool Material on Mechanical Properties of Friction Stir Welding," *Materials Today: Proceedings* 38 (2021).

[23] M. P. Mubiayi and E. T. Akinlabi, "Evolving Properties of Friction Stir Spot Welds Between AA1060 and Commercially Pure Copper C11000," *Transactions of Nonferrous Metals Society of China* 26, no. 7 (2016): 1852–1862, https://doi.org/10.1016/S1003-6326(16)64296-6

[24] Chee Kuang Kok, Mohammad Kamil Sued, Kia Wai Liew, *et al*., "Micro-Friction Stir Lap Welding (µFSLW) of Aluminum and Copper: A Short Review," *Engineering, Technology & Applied Science Research* 15, no. 2 (2025): 22004–22014, https://doi.org/10.48084/etasr.9650

[25] A. Bhatia, R. Wattal, R. Kumar, *et al*., "Optimization of Friction Stir Welding Parameters for Enhanced Mechanical Properties of AISI 1018 Carbon Steel," *Scientific Reports* 15 (2025): 31632, https://doi.org/10.1038/s41598-025-16668-0